

ROSAT and ASCA observations of X-ray luminous starburst galaxies: NGC 3310 and 3690

A. L. Zezas,¹ I. Georgantopoulos² and M. J. Ward¹

¹Department of Physics and Astronomy, University of Leicester, Leicester LE1 7RH

²National Observatory of Athens, Lofos Koufou, Palaia Penteli, 15236 Athens Greece

Accepted 1998 June 28. Received 1998 June 3; in original form 1997 December 30

ABSTRACT

We present *ROSAT* [High Resolution Imager (HRI) and Position Sensitive Proportional Counter (PSPC)] and *ASCA* observations of the two luminous ($L_x \sim 10^{41-42}$ erg s⁻¹) star-forming galaxies NGC 3310 and 3690. The HRI shows clearly that the sources are extended with the X-ray emission in NGC 3690 coming from at least three regions. The combined 0.1–10 keV spectrum of NGC 3310 can be described by two components, a Raymond–Smith plasma with temperature $kT = 0.81_{-0.12}^{+0.09}$ keV and a hard power law, $\Gamma = 1.44_{-0.11}^{+0.20}$ (or alternatively a harder Raymond–Smith plasma with $kT \sim 15$ keV), while there is no substantial excess absorption above the Galactic column value. The soft component emission is probably a super wind while the nature of the hard emission is more uncertain with the likely origins being X-ray binaries, inverse Compton scattering of infrared photons, an active galactic nucleus or a very hot gas component ($\sim 10^8$ K). The spectrum of NGC 3690 is similar, with $kT = 0.83_{-0.04}^{+0.02}$ keV and $\Gamma = 1.56_{-0.11}^{+0.11}$. We also employ more complicated models such as a multi-temperature thermal plasma, a non-equilibrium ionization code or the addition of a third softer component, which improve the fit but not at a statistically significant level ($< 2\sigma$). These results are similar to recent results on the archetypal star-forming galaxies M82 and NGC 253.

Key words: galaxies: individual: NGC 3690 – galaxies: individual: NGC 3310 – galaxies: interactions – galaxies: starburst – X-rays: galaxies.

1 INTRODUCTION

Significant X-ray emission from star-forming galaxies has been known since the *EINSTEIN* epoch (e.g. Stewart et al. 1982). Their X-ray spectrum in the 0.3–3.5 keV band can be fitted by a thermal plasma of temperature about 2 keV with an absorption often higher than the Galactic value (e.g. Fabbiano 1988; Kim, Fabbiano & Trinchier: 1992). However, simple spectral fits suggested that the emission mechanism may be more complicated than a single temperature thermal plasma. Indeed, for a few nearby star-forming galaxies (e.g. M82 and NGC 253) several discrete sources, mostly X-ray binaries, are also resolved (Long & Van Speybroeck 1983). The *EINSTEIN* HRI provided the first evidence for extended X-ray features (e.g. Watson, Stanger & Griffiths 1984; Fabbiano & Trinchier: 1984).

The effective area of *ROSAT* PSPC provided the opportunity to dramatically increase the number of star-forming galaxies studied in X-rays. Hot gas haloes and outflows, have also been observed, around many star-forming galaxies (e.g. Read, Ponman & Wolstencroft 1995; Della Ceca, Griffiths & Heckman 1997; Read, Ponman & Strickland 1997), as was anticipated based on previous optical (Heckman, Armus & Miley 1990) and theoretical work (e.g. MacLow and McCray 1988). This wind can be produced by the

supply of mechanical energy via stellar winds from evolved massive stars and numerous supernovae. The hot gas is accelerated outwards forming an expanding superbubble, which on reaching the extent of the minor axis of the galaxy, blows out following the onset of the Rayleigh–Taylor instability. These outflows can extend for several kpc along the minor axis of the galaxy, and have major influence on its subsequent evolution. This is especially so in the case of dwarf galaxies, where because of their weak gravitational potential, the wind can remove the interstellar medium causing star formation to cease, (e.g. Dekel & Silk 1986; Heckman et al. 1995). Combined *ROSAT* and *ASCA* observations of star-forming galaxies, (e.g. Serlemitsos, Ptak & Yaqoob 1996) suggest that the soft X-ray band can be fitted with a thermal plasma and a power-law model. The plasma temperature is ~ 0.6 – 0.8 keV, with an absorbing column $N_H > 10^{21}$ cm⁻², well above the Galactic value, and the power-law photon index is ~ 1.7 . The hard X-ray band can be fitted equally well with a high-temperature thermal plasma model, $kT > 6$ keV, (cf. Ohashi et al. 1990). The soft emission may emanate from the super-wind while the origin of the harder power-law X-ray emission may be a result of either X-ray binaries or inverse Compton scattering of infrared photons by the relativistic electrons generated by the supernovae (e.g. Rieke et al. 1980). The

Table 1. The X-ray luminous starburst galaxies in the Ho et al. sample.

Galaxy	X-ray luminosity [†] (erg s ⁻¹)
M82	40.88
NGC 3310	40.89
NGC 3690	41.62
NGC 4449	39.24
NGC 5204	39.54
NGC 5905	42.18 [‡]

[†] This is the log of the X-ray luminosity in the *ROSAT* band, from the RASS data.

[‡] This galaxy has show significant long time variability (Bade, Komossa & Dahlem 1996); this luminosity refers to the outburst epoch.

presence of very hot gas ($\sim 10^8$ K), or a weak active nucleus cannot be ruled out. However, medium spectral resolution, wide energy band (0.5–10 keV) observations of NGC 253 and M82 with *ASCA*, show that the above two-component models do not give an acceptable description of the data (Ptak et al. 1997; Moran & Lehnert 1997). Even the introduction of a third thermal component ($kT \sim 0.3$ keV) still provides a poor fit to the high-resolution *ASCA* SIS spectrum (Moran & Lehnert 1997). This suggests that the emission mechanisms are more complex than these simple models can explain. Since the X-ray spectra of Galactic supernova remnants (e.g. Hughes & Singh 1994) cannot be well-fitted by a simple Raymond–Smith model (their emission is dominated by non-equilibrium processes) it is likely that we are dealing with a similar situation in starforming galaxies.

One of the interesting results of the *ROSAT* All-Sky Survey was the discovery of star-forming galaxies with X-ray luminosities $\sim 10^{42}$ erg s⁻¹, approaching those of Seyfert galaxies (e.g. Moran, Halpern & Helfand 1996). In order to gain further insight into the nature of this powerful X-ray emission and to compare starburst properties with those of the archetypal (less luminous) star-forming galaxies, we have cross-correlated the *ROSAT* All Sky Survey Bright Source Catalogue, RASSBSC, (Voges et al. 1996) with the spectral atlas of nearby galaxies of Ho, Filippenko & Sargent (1995). The advantage of the latter sample is that it has high-quality optical spectra and thus provides us with a reliable classification for each galaxy. The sample of Ho et al. contains galaxies with declination $\delta > 0^\circ$ and magnitude $B < 12.5$ while the RASS contains almost 20 000 sources over the whole sky. The cross-correlation yielded 43 X-ray counterparts within 1 arcmin of the optical galaxy, whereas less than one coincidence is expected by chance. Within this sample of galaxies the vast majority are AGNs (Seyferts 1&2, and LINERS), but there are also some star-forming galaxies and high-luminosity early-type galaxies. Further details of the properties of the resulting X-ray sample are given elsewhere (Roberts 1998). The star-forming galaxies are listed in Table 1. In this Paper we present X-ray imaging and spectral analysis for the two most luminous star-forming galaxies in the sample: NGC 3310 and 3690, excluding NGC 5905 which underwent some form of transient phenomenon as yet not understood. Both *ROSAT* and *ASCA* observations are available in the HEASARC archive for these two galaxies.

We use a value of $H_0 = 50$ km s⁻¹ Mpc⁻¹ for the Hubble constant, throughout this paper. All errors quoted refer to the 90 per cent confidence level.

1.1 NGC 3310

NGC 3310 is a well-studied nearby galaxy of Sbc(r)pec type

(Mulder & Van Driel 1996). Its recession velocity is 980 km s⁻¹ (de Vaucouleurs et al. 1991) which implies a distance of 19.6 Mpc. Its optical image shows some interesting features. The most prominent is an arc and bow structure which extends for 100 arcsec to the northwest of the centre of the galaxy. Bertolla & Sharp (1984) propose that the arc could be part of a spiral arm and the bow is the remnant of an old jet. Balick & Heckman (1981) suggest that the whole structure is the remnant of a collision between the galaxy and a dwarf companion. This is in agreement with the suggestion of Mulder & Van Driel (1986) who characterize the system as a young merger based on the anomalies found in its rotation curve. It should be noted that in the radio and near-infrared images we do not see two resolved nuclei (Telesco & Gatley 1984; Balick & Heckman 1981). This could mean that the merger phase is now complete as suggested by Balick & Heckman.

Another interesting morphological feature is a giant H II region situated ~ 12 arcsec southwest of the nucleus (Balick & Heckman 1981). Its size is comparable to the largest extra galactic H II regions known, and its spectral characteristics are dominated by signatures of Wolf Rayet stars (Pastoriza et al. 1993).

The starburst nature of the activity has been confirmed by numerous observations in many spectral bands (e.g. Telesco & Gatley 1984; Smith et al. 1996; Balick & Heckman 1981). Evolutionary synthesis models of the starburst give an estimated age range of 10^7 to 10^8 years (Van der Kruit & de Bruyn 1976; Balick & Heckman 1981; Telesco & Gatley 1984; Pastoriza et al. 1993).

NGC 3310 has been previously observed with the Imaging Proportional Counter (IPC) on board the *EINSTEIN* observatory (Fabianno, Kim & Trinchieri 1992) yielding an X-ray flux $f_x = 1.1 \times 10^{-12}$ ergs⁻¹ cm⁻² in the 0.3–3.5 keV band for a 5-keV bremsstrahlung model and Galactic absorption. This corresponds to an X-ray luminosity of 5.0×10^{40} erg s⁻¹.

1.2 NGC 3690

NGC 3690 is also a merging system, but in contrast to NGC 3310 it is in an earlier merger phase. The system is composed of NGC 3690, which is the western part of the merger and IC694, the eastern component. The whole system is also known as Arp 299 or Mrk 171. Casoli et al. (1989) propose that there is a third component in the system thus forming an interacting triplet. Its recession velocity is 3159 km s⁻¹ (Sanders & Mirabel 1985), implying a distance of 63.2 Mpc. At that distance the projected separation of 22.5 arcsec of the two components corresponds to 6.9 kpc. The infrared surface brightness of NGC 3690 is at least twice that of IC694 (Friedman et al. 1987). The total mass of gas calculated from radio observations is about $2 \times 10^{11} M_\odot$ (Casoli et al. 1989).

The high IR luminosity ($L_{\text{FIR}} = 1.2 \times 10^{12} L_\odot$) (Soifer et al. 1987), results from re-radiating dust heated by the starburst activity. This is supported by multi-wavelength studies (Gehrz, Sramek & Weedman 1983; Friedman et al. 1987; Nakagawa et al. 1989). Detailed analysis of emission line ratios using the diagnostic diagrams of Veilleux & Osterbrock (1987) clearly indicate a stellar origin of the ionizing continuum (Friedman et al. 1987). The infrared emission is extended over a region of several kpc, but the main sources are located close to the two nuclei (Friedman et al. 1987). Modelling of the starburst has been carried out by Gehrz et al. (1983) and Nakagawa et al. (1989). The latter find a starburst age of about 10 Myr. An interesting point is that the two nuclei have different properties, implying either a different age and/or a different initial mass function (IMF) for each starburst event.

NGC 3690 has been previously observed with the High

Resolution Imager (HRI) onboard the *Einstein* observatory. 17 counts were detected implying an X-ray flux $f_x = 4.8 \times 10^{-13} \text{ erg s}^{-1} \text{ cm}^{-2}$ in the 0.2–4.0 keV band, for a 5-keV bremsstrahlung model and Galactic absorption (Fabianno et al. 1992). This corresponds to an X-ray luminosity of $2.3 \times 10^{41} \text{ erg s}^{-1}$.

2 OBSERVATIONS AND DATA REDUCTION

2.1 The ROSAT PSPC observations

NGC 3310 and 3690 were each observed on two occasions with the Position Sensitive Proportional Counter (PSPC) (Pfefferman et al. 1988) on board *ROSAT* (Trümper et al. 1984). The details of each observation are given in Table 2.

For the data reduction we have followed the standard procedure, using the *ASTERIX* package. We excluded those data with Master Veto rates higher than 170 count s^{-1} . We extracted a PSPC spectral image (channels 11 to 201) with a pixel size of 15 arcsec. To obtain an X-ray spectrum we extracted data from a circular region of 1.5-arcmin radius around the X-ray centroid. The background was estimated from an annular region between radii of 15 and 8.8 arcmin from the centroid, after exclusion of all the discrete sources detected with the PSS algorithm (Allen 1992) down to the 5σ level.

2.2 The ROSAT HRI observations

Both galaxies have been observed with the High Resolution Imager (HRI) (David et al. 1997) on board *ROSAT*. HRI covers a field of 38-arcmin diameter and it has a spatial resolution of about 5 arcsec (the FWHM of the XRT+HRI point spread function). We note that the HRI has very limited spectral resolution so we cannot use it for spectral analysis (David et al. 1997). The screening of the data has been carried out using the *ASTERIX* package. We have rejected all data with aspect errors greater than 2.

2.3 The ASCA observations

Both galaxies have been observed with the *ASCA* satellite (Tanaka, Inoue & Holt 1994). On board *ASCA* there are four instruments: two Gas Imaging Spectrometers (GIS2 and GIS3) (Ohashi et al. 1996) and two Solid-State Imaging Spectrometers (SIS0 and SIS1) (Gendreau 1995). For screening of the data we have followed the standard procedure and used the *ASCACLEAN* program in the *FTOOLS* package with the parameters described in the *ABC ASCA Guide*

(Yaqoob et al. 1997). After the standard processing we inspected the light curves and removed time intervals with unusually high numbers of counts, which may result from background particle contamination. The extraction of the source and the background spectra was carried out using the *XSELECT* program within the *FTOOLS* package. We extract the source spectrum using a circular region of 2.7 and 5.5 arcmin radius for the SIS and GIS respectively. For the background regions we have selected 10 source free zones, each of area about 6 and 10 arcmin² for the SIS and GIS respectively. Following extraction of the source and background spectra, we ran the *SISRMG* program to create the SIS response matrices for each SIS source spectral file. For the GIS spectral files we used the *gis2v4_0.rmf* and *gis3v4_0.rmf* for GIS2 and GIS3 respectively. We created the Ancillary Response Matrices for each file by running the *ASCAARF* programs within the *FTOOLS* package.

3 SPATIAL EXTENT ANALYSIS

3.1 NGC 3310

We used the archival *HRI* observations to obtain information on the morphology of the X-ray emitting regions and compared these with images of these galaxies at other wavelengths. First we searched for extended emission by comparing the background subtracted radial profile of the galaxies with the radial profile of a point source. For this purpose we used as a reference the point source corresponding to the star AR-Lac. We retrieved archival data for a non-axis observation of AR-Lac, and applied the same extraction process as used for the galaxy. The comparison of the radial profiles of NGC 3310, and the radial profile of AR-Lac is shown in Fig. 1. This figure clearly shows that the X-ray source has a radius of ~ 0.5 arcmin (at larger radii the emission from the galaxy begins to blend with the profile of AR-Lac, within the 2σ error bars). Although this is a somewhat arbitrary point at which to define the extent of the emission, it gives a lower limit to the source size. At the distance of NGC 3310 this corresponds to ~ 3 kpc. We note that fitting a Gaussian function to the radial profile gives a similar source size (FWHM = 1.6 arcmin).

In order to compare the distribution of the X-ray emitting gas with the optical image we have resampled the X-ray image with a pixel size of 1.5 arcsec and then smoothed this image using a two-dimensional Gaussian of FWHM = 3.5 arcsec (2.3 pixels) following Della Ceca et al. (1996). The final pixel size is 5.4 arcsec, equal to the XRT+HRI PSF. Then we obtained contours from this image corresponding to 2.2, 2.0, 1.7, 1.33, 0.88, 0.44, 0.35, 0.26, 0.17 count arcsec⁻² and overlaid these onto an optical image obtained

Table 2. Summary of the observations.

Galaxy	Satellite	Instrument	Date Observation started	Exposure Time ks
NGC 3310	<i>ROSAT</i>	PSPC	1991-11-16	9.114
	<i>ROSAT</i>	HRI	1995-04-17	41.842
	<i>ROSAT</i>	HRI	1994-11-23	4.095
	<i>ASCA</i>		1994-04-17	GIS: 10.4, SIS:10.4
	<i>ASCA</i>		1994-11-13	GIS:11.6, SIS:10.2
NGC 3690	<i>ROSAT</i>	PSPC	1993-04-22	3.534
	<i>ROSAT</i>	PSPC	1991-11-18	6.391
	<i>ROSAT</i>	HRI	1993-04-18	6.751
	<i>ASCA</i>		1994-04-06	GIS:5.7, SIS:5.3
	<i>ASCA</i>		1994-12-01	GIS:38.2, SIS:35.5

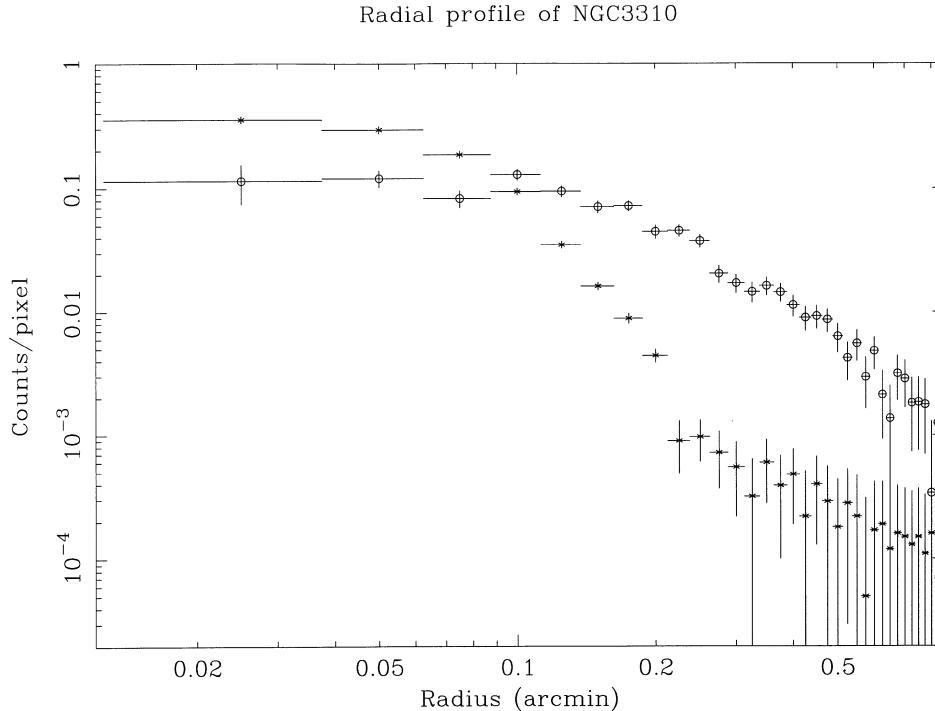


Fig. 1. The HRI radial profile of NGC 3310 (circles) overlaid on the radial profile of AR Lac (stars).

from the Digitized Sky Survey. This image is shown in Fig. 2. The main problem we faced in attempting to overlay the two images is that of frame registration. There are no X-ray sources within the HRI image which have an obvious optical counterpart. Thus in order to overlay the X-ray contour plot onto the optical image, we are forced to assume that the centroid of the X-ray source corresponds to that of the optical nucleus. In the X-ray image of NGC 3310 we detect two other sources in addition to the nucleus, at a significance above 10σ . The details concerning these sources are presented in Table 3. These point sources may correspond to luminous X-ray binaries or young supernova remnants. Unfortunately there are no identified optical counterparts for these X-ray sources on the POSS plates.

3.2 NGC 3690

The HRI analysis of NGC 3690 followed the same procedure as for NGC 3310. The image pixels were binned to a size of 1.5 arcsec and then smoothed using a two-dimensional Gaussian of FWHM 3.5 arcsec. Finally, we overlaid the X-ray contours on a POSS plate image obtained from the Digitized Sky Survey, Figure 3; the contours correspond to 0.57, 0.44, 0.40, 0.35, 0.31, 0.27, 0.22, 0.18, 0.13 and 0.11 count arcsec⁻² respectively. The most striking feature is the existence of three separate sources in the X-ray image. The two most luminous sources correspond to the two merging nuclei. Their X-ray fluxes are given in Table 4. The third X-ray source corresponds to a hot spot seen in the infrared and radio images to the north of NGC 3690 (the western component). Apart from these three sources there are marginal detections of other sources, but at a low level of significance (below 3σ), and will not be discussed further. We note that the relative strengths of the three main X-ray sources follow quite well the relative strengths of the near infrared sources, suggesting a possible common origin for the IR and the X-ray emission.

We have searched for extended emission from the two resolved

nuclei. From Fig. 3 it is clear that the emission from the two resolved nuclei is extended and not symmetrical. Fitting a Gaussian function to the radial profiles of NGC 3690 and IC694 yields a FWHM of 1.5 and 1.8 arcmin respectively.

Comparison between the X-ray images and radio (VLA-A observation of the H92 α radio recombination line, Zhao et al. 1997) and near-IR images (Wynn-Williams et al. 1991), available in the literature, shows some clear similarities. As the radio and near-IR emission is clearly associated with the star-forming regions, the spatial coincidence implies that the soft X-ray emission has its origin in the starburst. We note that we do not see any evidence of X-ray emission from hot connecting the two galaxies, unlike the situation in some other interacting star-forming galaxies (e.g. the Antennae, Fabbiano & Schweizer & Mackie 1997).

4 SPECTRAL ANALYSIS

We fitted all the datasets simultaneously, thus covering an energy range from 0.1 to 8.0 keV. We rejected all *ROSAT* PSPC data points below 0.1 and above 2.0 keV; and used only the SIS and GIS data in the range 0.6 to 8.0 keV and from 0.7 to 7.0 keV respectively. In order to apply χ^2 statistics we re-binned the spectra so as to contain at least 20 counts per bin. We used the software package XSPEC (v10) to obtain the spectral fits.

4.1 NGC 3310

We first fitted simple one-component models: a thermal bremsstrahlung model, a power-law model and finally a Raymond–Smith plasma model (Raymond & Smith 1977). These models were rejected at greater than the 99.9 per cent confidence level. The results of the spectral fits are given in Table 5.

We then fitted two-component models: a two-temperature Raymond–Smith plasma (ray-ray hereafter) and a Raymond–Smith plasma combined with a power-law (po-ray), following the

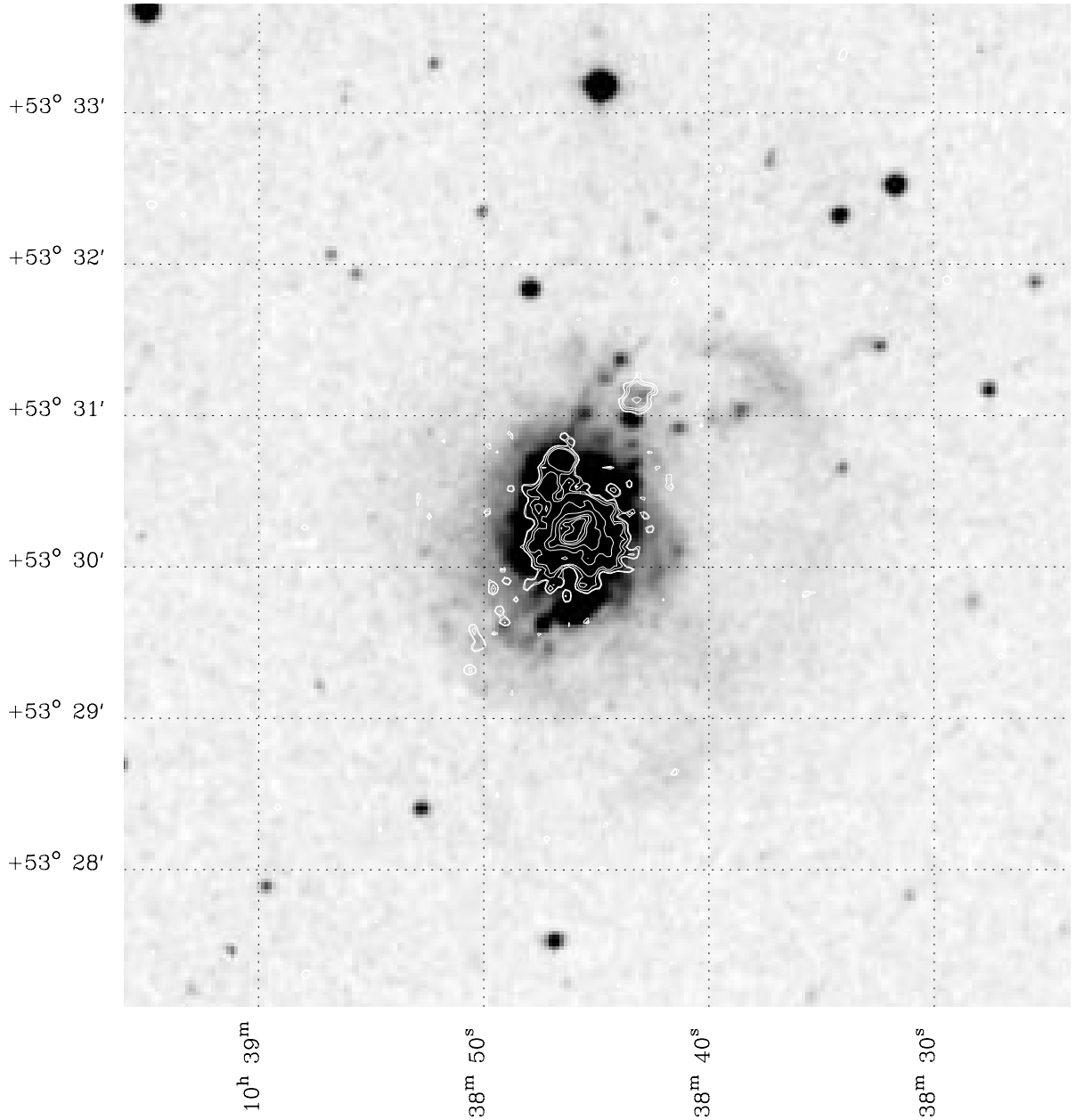


Fig. 2. X-ray contours from the HRI observation of NGC 3310 overlaid on a POSS image. The contours are in levels of 2.2, 2.0, 1.7, 1.33, 0.88, 0.44, 0.35, 0.26, 0.17 count arcsec⁻².

results of Moran & Lehnert (1997) and Ptak et al. (1997) on the starburst galaxies M82 and NGC 253. These models provided a much better fit than the simple models described above, at a confidence level over 90 per cent for an addition of two free parameters (e.g. Bevington & Robinson 1992). We consider first the po-ray model. We obtained a photon index of $\Gamma = 1.44^{+0.20}_{-0.11}$ and a temperature of $kT = 0.81^{+0.09}_{-0.12}$ keV with a reduced $\chi^2 = 1.115$, where the abundance is fixed to the solar value and the absorbing column density to the Galactic value, $N_{\text{H}} = 0.7 \times 10^{20} \text{ cm}^{-2}$ (Stark

et al. 1992). Leaving the absorbing column density as a free parameter further improves the fit (reduced $\chi^2 = 1.031$); this is significant at a confidence level of > 99 per cent for one additional parameter. In contrast, leaving the abundance as a free parameter does not improve the fit further at a statistically significant level.

In the ray-ray case we do not obtain a significantly improved fit compared to the po-ray model (reduced $\chi^2 = 1.022$). Fig. 4 shows the spectrum of NGC 3310 with the double Raymond–Smith model. We obtained temperatures of $0.80^{+0.07}_{-0.04}$ keV and

Table 3. Sources in the HRI field of NGC 3310.

RA (J2000)			Dec (J2000)			Count rate	Flux	Significance
10 ^h	38 ^m	43.2	+53°	31′	07″	$2.0 \pm 0.27 \times 10^{-3}$	2.3×10^{-14}	15.5
10	38	46.7	+53	30	38	$2.8 \pm 0.26 \times 10^{-3}$	3.07×10^{-14}	23.4

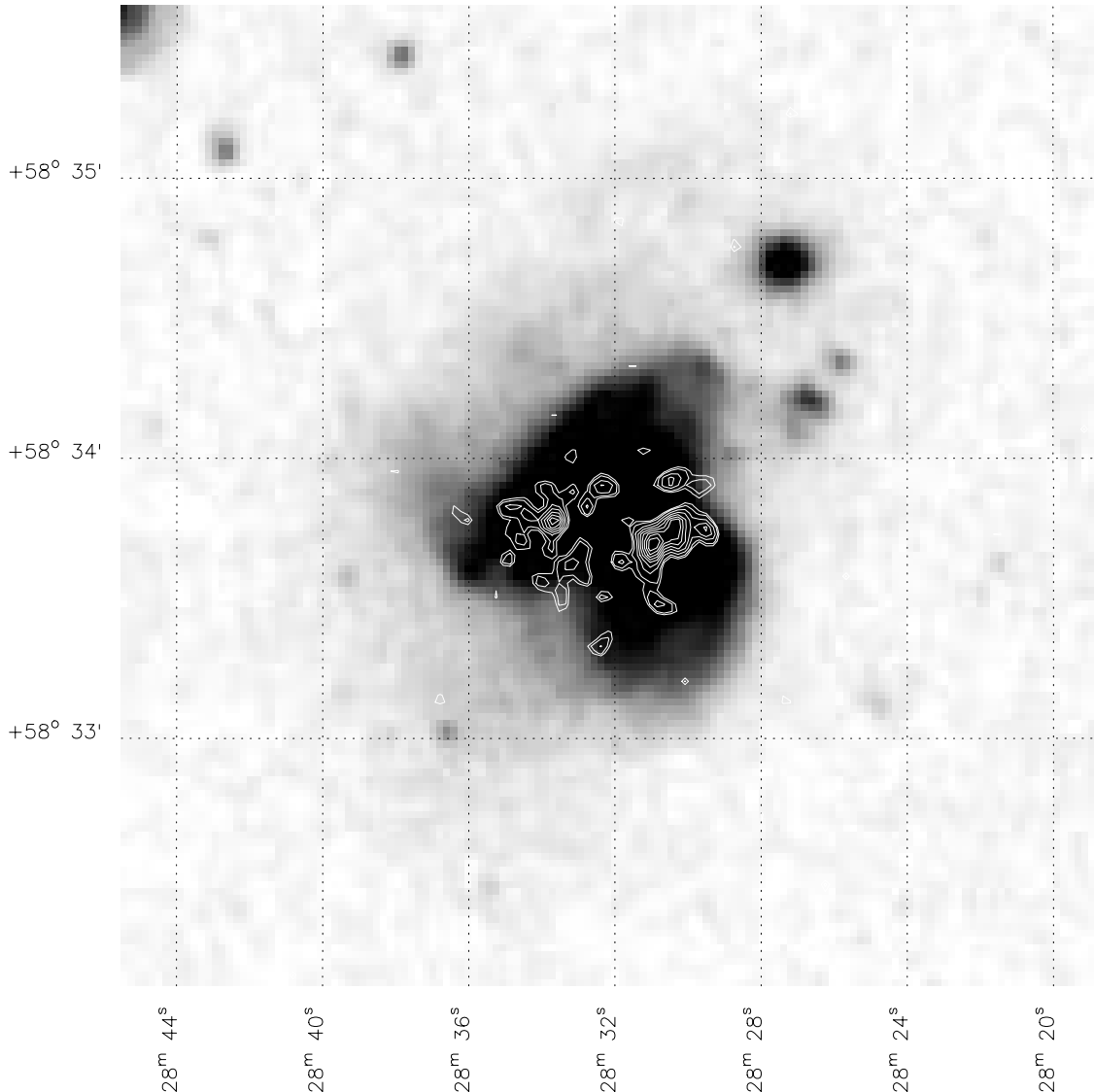


Fig. 3. X-ray contours from the HRI observation of NGC 3690 overlaid on a POSS image. The contours are in levels of 0.57, 0.44, 0.4, 0.35, 0.31, 0.26, 0.22, 0.18, 0.13, 0.11 count arcsec⁻².

14.98^{+13.52}_{-4.88} keV for an absorbing hydrogen column density of $N_{\text{H}} = 1.37^{+0.50}_{-0.32} \times 10^{20} \text{ cm}^{-2}$. When we fixed the column density to the Galactic value ($N_{\text{H}} \approx 1.0 \times 10^{20} \text{ cm}^{-2}$) we obtained $0.84^{+0.05}_{-0.07}$ and $kT \approx 64$ keV (which is unrealistically high). We also introduced two different absorbing column densities, for the soft and the hard components, following the analysis of M82 by Moran & Lehnert (1997) who showed that the hard X-ray component is obscured at the nucleus by $N_{\text{H}} \sim 10^{22} \text{ cm}^{-2}$. However, we do not find similar evidence here, since the hard component column has a value of $N_{\text{H}} \approx 1.77 \times 10^{20} \text{ cm}^{-2}$. Finally, we attempted to measure the element abundance in order to compare it with that for other

star-forming galaxies (Sansom et al. 1996; Serlemitsos et al. 1996), which appear to show a systematic trend towards sub-solar abundances. Unfortunately the data for our galaxies are not able to set any useful constraint on the abundances.

We do not detect the FeK α line at 6.7 keV as would be expected for a hot thermal plasma. The low signal-to-noise data above ~ 5 keV, does not allow us to set a useful upper limit on the line equivalent width. The lack of a strong FeK line could be explained by lower than solar abundances, as is probably the case in other well-studied starbursts such as NGC 253 (Ptak et al. 1997) and the Antennae (Sansom et al. 1996).

Table 4. Sources in the HRI field of NGC 3690.

	RA (J2000)		Dec (J2000)		Count rate (cps)	Flux (0.1–2.5 keV)	
11 ^h	28 ^m	30:7	+58°	33'	50''	$10 \pm 1.2 \times 10^{-3}$	1.18×10^{-13}
11	28	34.1	+58	33	51	$15 \pm 1.5 \times 10^{-3}$	1.72×10^{-13}
11	28	30.0	+58	34	03	$3 \pm 0.6 \times 10^{-3}$	3.17×10^{-14}

Table 5. Spectral fitting results for NGC 3310.

Parameter	Power law	Single Temperature Raymond–Smith	Double Temperature Raymond–Smith	Raymond–Smith + Power law
kT (keV)		$7.35^{+1.24}_{-1.18}$	$0.80^{+0.07}_{-0.04}$ $14.98^{+13.52}_{-4.88}$	$0.81^{+0.09}_{-0.12}$
Γ	$1.68^{+0.08}_{-0.08}$			$1.44^{+0.20}_{-0.11}$
$N_{\text{H}}(10^{20} \text{ cm}^{-2})$	$3.15^{+0.63}_{-0.52}$	$1.90^{+0.45}_{-0.36}$	$1.37^{+0.50}_{-0.32}$	$1.74^{+0.68}_{-0.40}$
$\chi^2 / \text{d.o.f.}$	222.9/175	239.3/175	168.7/165	170.2/165
Flux [†] (0.1–2.0keV)	0.95	0.86	0.9	1.09
Flux [†] (2.0–10.0keV)	1.88	2.12	2.10	2.10
Total Luminosity [‡] (0.1–10keV)	1.3	1.4	1.4	1.5

[†]All the fluxes are in units of $10^{-12} \text{ erg s}^{-1} \text{ cm}^{-2}$.

[‡]The luminosity is in units of $10^{41} \text{ erg s}^{-1}$.

We note that a previous preliminary analysis of *ASCA* data by Serlemitsos et al. (1996), find a spectral slope consistent with our value. However, they derive a considerably higher column density, but without the benefit of using the lower energy *ROSAT* data.

4.2 NGC 3690

The spectral analysis follows the same procedures as for NGC 3310. Simple one-component models such as a power-law and a Raymond–Smith plasma are similarly rejected (see Table 6). Two-component models, such as a po-ray and a ray-ray model (with the hydrogen column density as a free component) give $\Gamma = 1.56^{+0.11}_{-0.11}$, $kT = 0.83^{+0.02}_{-0.04}$, $N_{\text{H}} = 2.4^{+0.6}_{-0.5} \times 10^{20} \text{ cm}^{-2}$ and $kT_1 = 0.83^{+0.03}_{-0.03}$, $kT_2 = 10.3^{+5.95}_{-2.44}$, $N_{\text{H}} = 1.6^{+0.4}_{-0.4} \times 10^{20} \text{ cm}^{-2}$ respectively (the Galactic absorption is $N_{\text{H}} = 1 \times 10^{20} \text{ cm}^{-2}$). In the above model the abundance was fixed to solar. Also, as for NGC 3310 when the abundance is a free parameter, it cannot be usefully constrained. Fig. 5 shows the *ROSAT* and *ASCA* spectrum of NGC 3690 with the best-fitting double temperature Raymond–Smith

thermal plasma model. We can clearly see from the spectrum that there is no evidence for an Fe line at $\sim 6.7 \text{ keV}$. The upper limit to the Fe line equivalent width is $\sim 860 \text{ eV}$. We also tried to fit the models using a different absorbing column for the hard component. We obtain $N_{\text{H}} = 1.7^{+0.1}_{-0.8} \times 10^{20} \text{ cm}^{-2}$, which is comparable to the previous best-fitting values, while the χ^2 is not significantly improved for one additional parameter. Thus there is no evidence for excess absorption in the hard component, in contrast to the results for M82 (Moran & Lehnert 1997). We also note that both the ray-ray and the po-ray models do not provide an adequate fit to the data as they can be rejected at over the 99 per cent level of confidence using a χ^2 goodness of fit.

We therefore attempted to fit more complicated models, such as multi-temperature components, and a power-law distribution of temperatures. This is model ‘cevmekl’ in *XSPEC*, (see Done & Osborne 1997). This model gives a best fit of reduced $\chi^2 = 1.286$, with a maximum cut-off in the temperature distribution of $\sim 57 \text{ keV}$, a power-law index of the temperature distribution of $\alpha = 0.22^{+0.11}_{-0.10}$ and $N_{\text{H}} = 3.21^{+0.73}_{-0.48} \times 10^{20} \text{ cm}^{-2}$. A combination of a

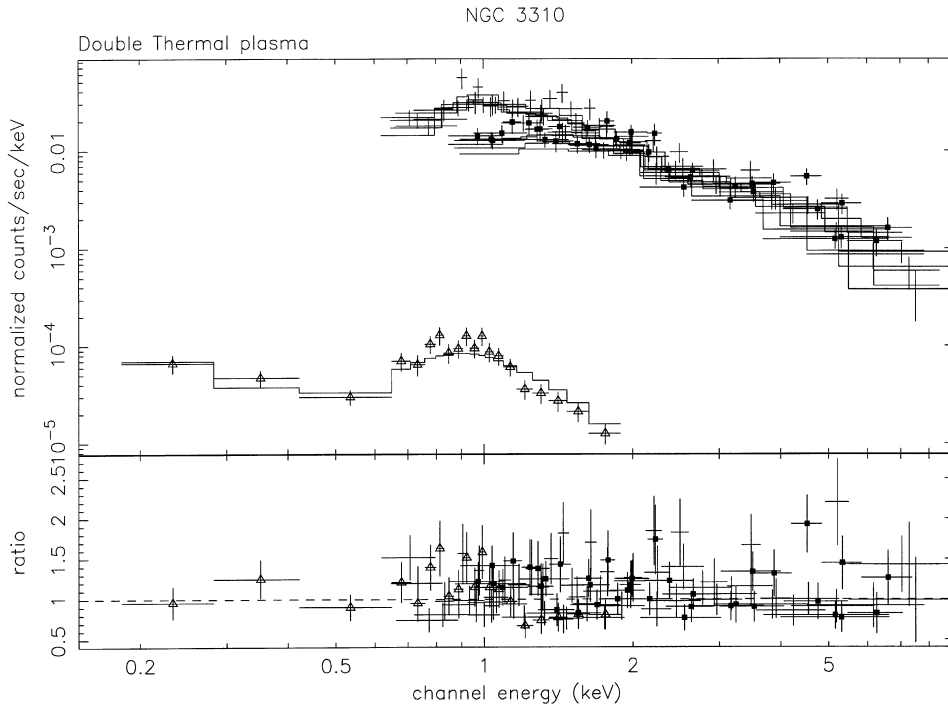


Fig. 4. The top panel shows *ROSAT* and *ASCA* spectra of NGC 3310 with the best-fitting double Raymond–Smith model. The bottom panel shows the ratio of the data points to the model. The SIS data are marked with dots while the PSPC data are marked with triangles.

Table 6. Spectral fitting results for NGC 3690.

Parameter	Power law	Single Temperature Raymond–Smith	Double Temperature Raymond–Smith	Raymond–Smith + Power-law	Triple temperature Raymond–Smith	cevmekl	cevmekl + power law
kT (keV)		$4.25^{+0.36}_{-0.45}$	$0.83^{+0.03}_{-0.03}$ $10.3^{+5.9}_{-2.4}$	$0.83^{+0.02}_{-0.04}$	$0.285^{+0.187}_{-0.063}$ $0.871^{+0.427}_{-0.676}$ $11.17^{+6.96}_{-3.13}$	57.08(> 30)	
Γ	$2.23^{+0.12}_{-0.12}$			$1.56^{+0.11}_{-0.11}$			$1.52^{+0.13}_{-0.12}$
α^\dagger						$0.22^{+0.11}_{-0.01}$	1.0
N_{H} (10^{20}cm^{-2})	$5.50^{+0.7}_{-0.7}$	$2.11^{+0.38}_{-0.33}$	$1.60^{+0.42}_{-0.40}$	$2.42^{+0.63}_{-0.46}$	$2.031^{+0.283}_{-0.472}$	$3.21^{+0.73}_{-0.48}$	$2.91^{+0.68}_{-0.55}$
$\chi^2 / \text{d.o.f.}$	490.0/242	624.5/242	287.8/235	291.5/235	290.3/237	309.9/241	286.4/235
Flux ‡ (0.1–2.0keV)	9.72	8.85	8.5	9.0	8.95	8.62	8.2
Flux ‡ (2.0–10.0keV)	7.68	9.59	10.8	10.8	10.3	9.9	10.8
Total Luminosity* (0.1–10.0keV)	8.3	8.8	9.2	9.46	9.2		

† The slope of power-law distribution of temperatures in the cevmekl model.

‡ The fluxes are in units of $10^{-13} \text{erg s}^{-1} \text{cm}^{-2}$.

* The luminosity is in units of $10^{41} \text{erg s}^{-1}$.

power-law and the multi-temperature model gives a slightly better fit (reduced $\chi^2 = 1.211$) with $\Gamma = 1.52^{+0.13}_{-0.12}$, $T_{\text{max}} = 1.17^{+0.25}_{-0.16}$ and α fixed to 1. Finally, we considered using a non-equilibrium-ionization model (NEI), such as that applied to hot gas resulting from supernova explosions (Hughes & Singh 1994). This model assumes that the gas is instantaneously shock heated, and then applies corrections to the Raymond–Smith thermal plasma code to account for the non-equilibrium ionization fraction. An additional variable in the NEI model is nt , which is the product of the electron density and the time elapsed since the passage of the shock wave. In principle the results from fitting NEI models can be used to estimate the characteristic time-scale over which the gas reaches ionization equilibrium. Clearly for a situation in which multiple supernova occur over an extended time period, it will not be possible to identify a unique time-scale. However, NEI models have been applied to the optically thin plasma in galactic-scale superwinds,

such as observed in M82, Tsuru et al. (1998). Unfortunately in the case of NGC 3690, we do not have the benefit of measurements of the low-energy lines of silicon and magnesium needed to quantify the importance of non-equilibrium effects. For NGC 3690 the NEI models give a best fit with a combination of a power-law and a NEI model. However the reduction in the χ^2 is not statistically significant at a level above 90 per cent, and so we conclude that our data does not justify further consideration of the NEI models. However, if new soft X-ray emission line data become available, it would be worthwhile returning to this question.

5 DISCUSSION

5.1 The soft X-ray emission

The HRI images clearly show the extended X-ray emission in both

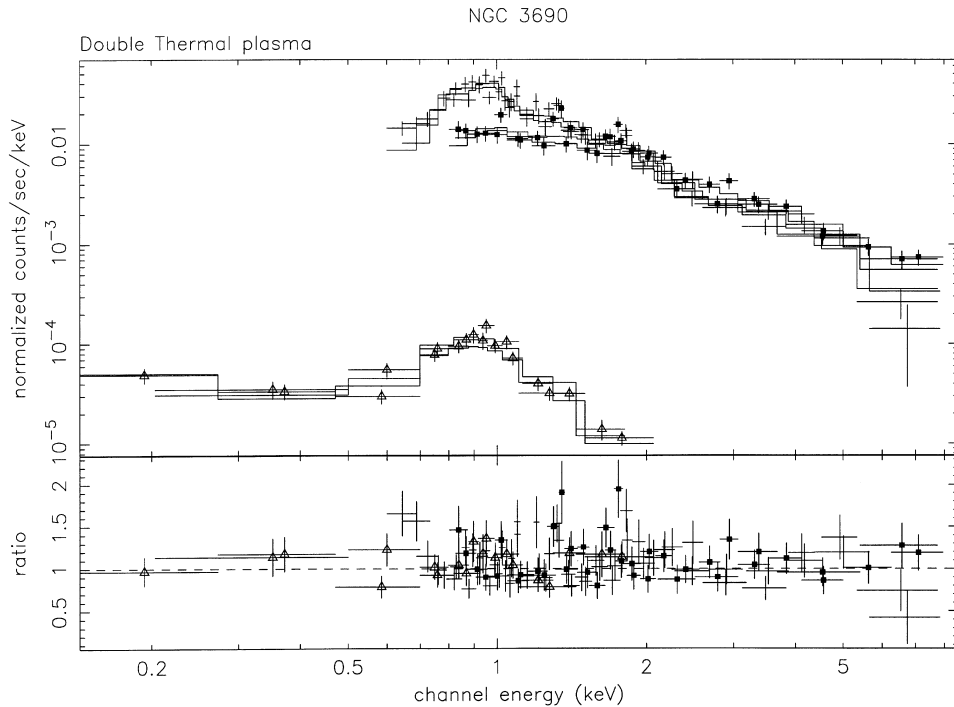


Fig. 5. The top panel shows *ROSAT* and *ASCA* spectra of NGC 3690 with the best-fitting double Raymond–Smith model. The bottom panel shows the ratio of the data points to the model. The SIS data are marked with dots, while the PSPC data are marked with triangles.

NGC 3310 and NGC 3690/IC694. This supports a thermal origin for the soft emission, which may be due to a galactic-scale super-wind e.g. Heckman et al. (1990). Such a phenomenon is observed in other star-forming galaxies, M82 (Strickland, Ponman & Stevens 1997), NGC 1569 (Della Ceca et al. 1996) and NGC 4449 (Della Ceca et al. 1997). According to this scenario, supernova in the starburst region create a hot ($\sim 10^8$ K) bubble. The dense shell around the bubble fragments owing to Rayleigh–Taylor instabilities and forms the optical emission line filaments and is probably a source of soft X-ray emission. The optical data also support this model. In the case of NGC 3690 the H α images show plumes and filaments extending out to several kpc (Armus, Heckman & Miley 1990). Additional evidence comes from the extended synchrotron radio emission which may arise from the electrons produced by supernova remnants in the starburst regions (Gehrz et al. 1983). In the case of NGC 3310 the situation is more complicated as its low inclination angle ($\theta \approx 32^\circ$) makes detection of any outflow along the minor axis of the galaxy very difficult.

In order to further test the validity of the above model, we can estimate the expected X-ray luminosity of the super-wind and compare this with the observed luminosity of the soft Raymond–Smith component. First we relate the X-ray luminosity of the gas contained in a superbubble with the basic properties of the starburst; its bolometric luminosity and age. Heckman et al. (1995) have calculated the total X-ray luminosity from a superbubble by integrating over its volume, and using the expressions for the gas density and the bubble radius derived by MacLow & McCray (1988). They find that $L_x \approx 5 \times 10^{39} L_{41}^{33/35} n^{17/35} t_7^{9/35} \text{ erg s}^{-1}$, where L_{41} is the injection rate of mechanical energy into the bubble in units of $10^{41} \text{ erg s}^{-1}$, n is the gas density and t_7 is the age of the bubble in units of 10 Myr. Considering that the formation of the bubble begins, as a result of strong winds from O stars following the starburst, we can assume that the age of the bubble is almost the same as the age of the starburst. Using the relation $dE/dt = 7 \times 10^{42} L_{\text{IR},11} \text{ erg s}^{-1}$, (Heckman et al. 1990) which correlates the total infrared luminosity (in units of $10^{11} L_\odot$) of a starburst with age greater than 10^7 yr with the kinetic energy deposition rate from supernovae and stellar winds, we can estimate the X-ray luminosity. Using the *IRAS* data from Soifer et al. (1987), the IR luminosity of NGC 3310 is $5.5 \times 10^{10} L_\odot$. Assuming a gas density of $\sim 1 \text{ cm}^{-3}$ and a typical starburst age of 10 Myr we obtain an X-ray luminosity $L_x = 1.5 \times 10^{41} \text{ erg s}^{-1}$ in the *ROSAT* band. This luminosity is larger than the measured luminosity in the same energy band ($L_x = 4.7 \times 10^{40} \text{ erg s}^{-1}$), but considering the large uncertainties in the model parameters involved, we conclude that the super-wind model remains a possible scenario for the origin of the soft X-ray emission. In NGC 3690/IC694 the situation is more complex, as there are at least three distinct starburst components (Nakagawa et al. 1989) which are unresolved by *IRAS*. In order to obtain an estimate of the mechanical energy input for each component, we used the ground based mid-IR data (10–32 μm) of Wynn-Williams et al. (1991). These observations have sufficient spatial resolution to separate the three components. We then make the reasonable assumption that the fractions of the total *IRAS* flux which arise from each of the three star-forming components, are similar to the fractions in the mid-IR band. Using the same formulae (Heckman et al. 1995) as in the analysis of NGC 3310 above, and assuming a starburst age of 10 Myr and a density of $n = 1 \text{ cm}^{-3}$, we predict $L_x = 1.3 \times 10^{42}$, 1.1×10^{42} and $3.2 \times 10^{41} \text{ erg s}^{-1}$ for the A, B and C components respectively (following notation of Gehrz et al. 1983). Again the predicted luminosity is higher than the measured soft (0.1–2.5 keV) X-ray luminosity ($4.7 \times 10^{41} \text{ erg s}^{-1}$). This could possibly result from the fact that

some fraction of the far-infrared emission measured by *IRAS*, may arise from regions more extended than those producing the X-rays. Another possibility is that an additional source of heating may be present, perhaps owing to stars of later spectral type than those producing the winds.

The soft X-ray spectra of NGC 3310 and 3690 are very similar. A Raymond–Smith component with a temperature of $kT \sim 0.8$ keV dominates the spectrum at soft energies and could originate from the super-wind. This temperature is similar to that found for other star-forming galaxies, e.g. M82 and NGC 253 (Ptak et al. 1997), NGC 1569 (Della Ceca et al. 1996), NGC 4449 (Della Ceca et al. 1997) NGC 6240 and 2782 (Schulz et al. 1997). In the case of NGC 3690 where the photon statistics are good, the SIS spectral fit yields a poor χ^2 fit. This could be suggestive of a hot tenuous gas component. Indeed, if the expanding gas has not had time to reach thermal equilibrium, its spectrum will not be well represented by the Raymond–Smith model. The use of a non-equilibrium code by Hughes et al. improved the fit, but again the χ^2 is not accepted at the 98 per cent confidence level. This is not surprising as even a non-equilibrium model may be inadequate to fit an ensemble of supernova remnants occurring in several star-forming regions as is the case for NGC 3690/IC694.

5.2 The hard X-ray emission

The spectrum at X-ray hard energies can be represented, in both galaxies, by a power law ($\Gamma \sim 1.4 - 1.6$), or alternatively by a Raymond–Smith component with high temperature, ($kT > 10$ keV). There is no strong evidence for the presence of a large amount of obscuration as is the case for NGC 253 and M82 (Ptak et al. 1997). There are at least four possibilities for the origin of the hard X-ray emission: (a) inverse Compton scattering of the IR photons produced in the starburst by electrons from the numerous supernova remnants (e.g. Schaaf et al. 1989); (b) emission from a low-luminosity AGN as is the case in NGC 3628 (Yaqoob et al. 1995); (c) thermal emission from a very hot gas ($T \sim 10^8$ K); (d) emission from X-ray binaries (Griffiths & Padovani 1990). We discuss each of these possibility in turn. We consider first the possibility, that the hard X-ray emission arises from inverse Compton (IC) scattering of the copious infrared photons off of the relativistic electrons generated by the numerous supernovae. Support for this, especially in the case of NGC 3310, comes from the similarity (within the errors) of the spectral index of the hard X-rays and the spectral index of the radio emission ($\alpha_{\text{rad}} = 0.61_{-0.03}^{+0.03}$, Niklas, Klein & Weilebinski 1997). Following Schaaf et al. (1989) we can estimate the X-ray luminosity from inverse Compton scattering. Unfortunately, we can perform this calculation only for NGC 3310, as there are no suitable radio data available for NGC 3690. From Vallée (1993) we have that the ‘minimum energy’ magnetic field (see Longair 1992) is $B = 0.47 \times 10^{-5} \text{ G}$. Then the minimum energy density is $u = (7/3)(B^2/8\pi) \text{ erg cm}^{-3} = 2.05 \times 10^{-12} \text{ erg cm}^{-3}$. Following Schaaf et al. (1989) we have that $L_{\text{IC}} = (1/3) \sigma_{\text{T}} R_{\text{IC}} L_{\text{IR}} (\epsilon_e/mc^2) \gamma_2^{0.8} \gamma_1^{0.2}$, where σ_{T} , R_{IC} , L_{IR} and mc^2 , ϵ_e are the Thomson cross-section, the thickness of the disc, the far-IR luminosity, the rest mass of the electron and the energy density of the relativistic electrons, respectively. For a typical galactic disc $R_{\text{IC}} \sim 1 \text{ kpc}$ (we cannot measure the actual thickness of the disc since NGC 3310 is almost face on) and for a typical value of the low-frequency cut-off $\nu = 0.01 \text{ GHz}$ we have $\gamma_1 = 150$ for the lower limit of the Lorentz factor, and $\gamma_2 = 10^3$ for the maximum Lorentz factor, in order to have IC emission at 10 keV (Schaaf et al.

1989). So for the Inverse Compton X-ray luminosity we predict a value of $2.5 \times 10^{38} \text{ erg s}^{-1}$, much lower than the detected hard X-ray luminosity of NGC 3310, thus implying that IC can be only a minor component of the total X-ray emission from this galaxy. We caution that this result is quiet uncertain as the calculation depends on parameters like the volume of the source and the thickness of the disc, which are poorly known. Another possible origin of the hard X-ray emission is the presence of a low-luminosity AGN, although there is no evidence for non-starforming nuclear activity from diagnostic emission line ratio diagrams based on optical and near infrared spectra.

However, the hard X-ray power-law spectrum is nevertheless consistent with the presence of an active nucleus. In order to test this possibility further we use the $L_x/L_{H\alpha}$ relation from Elvis, Soltan & Keel (1984), where $L_{H\alpha}$ is the luminosity of the broad component of the $H\alpha$ line and L_x is the hard X-ray luminosity (2–10 keV). $L_x/L_{H\alpha} \approx 40$, for low-luminosity AGN and thus we estimate $f(H\alpha) \sim 5.3 \times 10^{-14} \text{ erg s}^{-1} \text{ cm}^{-2}$ and $2.7 \times 10^{-14} \text{ erg s}^{-1} \text{ cm}^{-2}$ for NGC 3310 and 3690 respectively. A broad component of this strength is easily detectable, but is not seen (Ho, Filippenko & Sargent 1997). The absorbing columns found from the X-ray spectral fitting (ray-po models in Tables 5 and 6) imply low extinctions, $A_V \sim 0.1$ mag for both galaxies (Bohlin, Savage & Drake 1978). Hence a BLR reddened by this amount would still be observed.

The next possibly is the presence of a very hot thermal component. A Raymond–Smith model with $kT > 10$ keV provides a good fit to the data. However, the strong FeK line at 6.7 keV which should accompany the thermal emission is not observed. This could be attributed to a low metallicity, but unfortunately we cannot check this as the abundances are not well constrained using the present X-ray data. Alternatively, the lack of a FeK line could be explained by a low contribution of type Ia supernovae to the enrichment of the interstellar medium (Sansom et al. 1996).

Finally we consider high-mass X-ray binaries as a possible origin of the hard X-ray component. High-mass binaries will form as a consequence of the starburst, and indeed many such systems have been identified in nearby star-forming galaxies (Read, Ponman & Strickland 1997; Fabbiano 1995 and references therein). Assuming that a typical X-ray luminosity of these systems is $10^{37-38} \text{ erg s}^{-1}$, we can estimate the total number of binaries. As the X-ray luminosity of the hard component is $L_x \sim 5 \times 10^{41}$ and $L_x \sim 10^{41} \text{ erg s}^{-1}$ for NGC 3690 and 3310 respectively, we estimate a range of between 5000–50 000 and 1000–10 000 X-ray binaries for the two galaxies. Now we can compare this with the number of ionizing OB stars determined from the integrated far-infrared luminosity. Making the assumption that it is mostly these stars that heat the dust, which then reradiates in the mid-far infrared, we estimate $\sim 2 \times 10^5$ and $\sim 3.5 \times 10^6$ OB stars for NGC 3310 and 3690, respectively. If, following Fabbiano et al. (1992), 0.2 per cent of these are massive X-ray binaries, then there are 400, and 7000 such systems, respectively. For the upper range of binary luminosities the predicted X-ray luminosity is comparable to that observed in both cases. Indeed, if the hard X-ray emission arises from binaries with low metallicity and thus high X-ray luminosity ($L_x \sim 10^{38-39} \text{ erg s}^{-1}$) like those observed in the Magellanic Clouds (van Paradijs & McClintock 1995), then they could easily produce the observed luminosity. One potential problem is that some point sources observed in nearby galaxies with the *ROSAT* PSPC by Read et al. (1997), appear to have soft spectra ($kT \sim 2$ keV), whilst the the high temperatures inferred for NGC 3310 and 3690 are closer to those predicted for high mass X-ray binaries (see Nagase 1989).

6 CONCLUSIONS

We have modelled and interpreted the combined *ASCA* and *ROSAT* X-ray spectra from 0.1–10 keV, for the star-forming galaxies NGC 3310 and 3690. These two galaxies are amongst the most X-ray luminous ($L_x \sim 10^{41-42} \text{ erg s}^{-1}$) starbursts in the local Universe. In addition, *ROSAT* HRI images show that the emission from NGC 3310 is extended out to at least ~ 3 kpc. The soft X-ray emission from NGC 3690 comes from at least three spatially resolved regions. The limited spatial resolution of the *ASCA* data does not allow us to place useful limits on the extent of their hard X-ray components. The X-ray spectrum of NGC 3310 can be described by two components: at soft energies a Raymond–Smith component ($kT \sim 0.8$ keV) which probably originates from a super-wind. The predicted soft X-ray emission, on the basis of the supernovae mechanical energy deposited to the interstellar medium, is comparable to that observed. At harder energies we can fit either a Raymond–Smith component ($kT \sim 17$ keV) or a power law $\Gamma \sim 1.4$.

The results for NGC 3690 are similar. There are at least two components in its spectrum: a soft Raymond–Smith plasma ($kT \sim 0.8$ keV) and a harder component which can be represented equally well by a Raymond–Smith component ($kT \sim 10$ keV) or a hard power law $\Gamma \sim 1.6$. However, the best-fitting model for NGC 3690 is rejected at the 98 per cent confidence level implying that more complicated models are necessary. Hence we considered a non-equilibrium ionization model (Hughes & Singh 1994) and a multi-temperature thermal model (Done & Osborne 1997). The above models do improve the fit, but only at the ~ 90 per cent confidence level. Although non-equilibrium models may be important, additional information such as X-ray emission line ratios are required in order to make further quantitative progress.

In neither NGC 3310 and 3690 do we find evidence for significant absorption columns above the Galactic values, in either the soft or the hard X-ray component.

The nature of the hard X-ray emission is still uncertain, and we considered various possibilities. Of these we conclude that inverse Compton scattering by high-energy radio electrons and infrared photons, can probably provide only a minor contribution. Although the presence of an AGN is a possibility, this is not supported by data at other wavelengths, and the modest columns argue against an obscured nucleus. A very hot thermal component may be present, ($\sim 10^8$ K). We do not detect the FeK line at 6.7 keV, possibly because the abundances are sub-solar. To test this possibility further requires information on element abundances, and an extension of the observed spectra to higher energies. Finally, estimates of the number of X-ray binaries, based on the total mid-IR emission, suggests that they may well be able to account for the hard X-ray emission.

The X-ray results on these two galaxies are similar to those obtained for other dwarf star-forming galaxies (e.g. NGC 1569, NGC 4449) and the archetypal star-forming galaxies M82 and NGC 253, although there is a range in relative contributions from the various X-ray components. This implies that the same general emission mechanisms apply in star-forming galaxies over three decades of luminosity.

ACKNOWLEDGMENTS

We are grateful to J. Hughes for providing the supernova remnant non-equilibrium XSPEC model.

REFERENCES

- Allen D. J., 1992, *ASTERIX User Note 004*, Starlink
- Armus L., Heckman T. M., Miley G. K., 1990, *ApJ*, 364, 471
- Bade N., Komossa S., Dahlem M., 1996, *A&A*, 309, 35L
- Balick B., Heckman T., 1981, *A&A*, 96, 271
- Bertolla A. F., Sharp N. A., 1984, *MNRAS*, 207, 47
- Bevington P. R., Robinson D. K., 1992, *Data reduction and error analysis for the physical sciences*, 2nd edn. McGraw Hill, New York
- Bohlin R. C., Savage B. D., Drake J. F., 1978, *ApJ*, 224, 132
- Casoli F., Combes F., Augarde R., Figon P., Martin J. M., 1989, *A&A*, 224, 31
- David et al., 1997, *The ROSAT HRI Calibration Report*, http://hea-www.harvard.edu/rosat/rsdc/www/HRI_CAL_REPORT
- de Vacouleurs G. et al., 1991, *Third Reference catalogue of bright galaxies*.
- Dekel A., Silk J., 1986, *ApJ*, 303, 39
- Della Ceca R., Griffiths R. E., Heckman T. M., Mackenty J. W., 1996, *ApJ*, 469, 662
- Della Ceca R., Griffiths R. E., Heckman T. M., 1997, *ApJ*, 485, 581
- Done C. D., Osborne J. P., 1997, *MNRAS*, 288, 649
- Elvis M., Soltan A., Keel W., 1984, *ApJ*, 283, 479
- Fabbiano G., 1988, *ApJ*, 3310, 672
- Fabbiano G., 1995, in Lewin W. H., van Paradijs J., van den Heuvel E. P. J., eds, *X-ray Binaries*. Cambridge Univ. Press, Cambridge
- Fabbiano G., Trinchieri G., 1984, *ApJ*, 286, 491
- Fabbiano G., Kim D. W., Trinchieri G., 1992, *ApJS*, 80, 531
- Fabbiano G., Schweizer F., Mackie G., 1997, *ApJ*, 478, 542
- Friedman S. D., Cohen R. D., Jones B., Smith H.E., Stein W. A., 1987, *AJ*, 94, 1480
- Gehrz R. D., Sramek R. A., Weedman D. W., 1983, *ApJ*, 267, 551
- Gendreau K. C., 1995, PhD thesis
- Griffiths R. E., Padovani P., 1990, *ApJ*, 360, 483
- Heckman T. M., Armus L., Miley G. K., 1990, *ApJS*, 74, 833
- Heckman T. M., Dahlem M., Lehnert M. D., Fabbiano G., Gilmore D., Waller W. H., 1995, *ApJ*, 448, 98
- Ho L. C., Filippenko A. V., Sargent W. L., 1995, *ApJS*, 98, 477
- Ho L. C., Filippenko A. V., Sargent W. L. W., 1997, *ApJS*, 112, 315
- Hughes J. P., Singh K. P., 1994, *ApJ*, 422, 126
- Kim D. W., Fabbiano G., Trinchieri G., 1992, *ApJS*, 80, 645
- Long K. S., van Spreybroeck L. P., 1983, in Lewin W. H. G., van den Heuvel E. P. J., eds, *Accretion driven stellar X-ray sources*. Cambridge Univ. Press, Cambridge
- Longair M. S., 1992, *High Energy Astrophysics*, Vol.2. Cambridge Univ. Press, Cambridge
- MacLow M. M., McCray R., 1988, *ApJ*, 324, 776
- Moran E. C., Halpern J. P., Helfand D. J., 1996, *ApJS*, 106, 341
- Moran E. C., Lehnert M. D., 1997, *ApJ*, 478, 172
- Mulder P. S., Van Driel W., 1996, *A&A*, 309, 403
- Nagase F., 1989, *PASJ*, 41, 1
- Nakagawa T., Nagata T., Geballe T. R., Okuda H., Shibai H., Matsuhara H., 1989, *ApJ*, 340, 729
- Niklas S., Klein U., Weilebinski R., 1997, *A&A*, 322, 19
- Ohashi et al., 1990, *ApJ*, 365, 180
- Ohashi et al., 1996, *PASJ*, 48, 157
- Pastoriza M. G., Dottori H. A., Terlevich E., Terlevich R., Diaz A. I., 1993, *MNRAS*, 260, 177
- Pfefferman et al., 1988, *Proc. SPIE*, 733, 519
- Ptak A., Serlemitsos P., Yaqoob T., Mushotzky R., Tsuru T., 1997, *AJ*, 113, 1286
- Raymond J. C., Smith B. W., 1977, *ApJS*, 35, 419
- Read A. M., Ponman T. J., Strickland D. K., 1997, *MNRAS*, 286, 626
- Read A. M., Ponman T. J., Wolstencroft R. D., 1995, *MNRAS*, 277, 397
- Roberts T., 1998, PhD thesis, Univ. Leicester
- Rieke G. H., Lebofsky M. J., Thompson R. I., Low F. J., Tokunaga A. T., 1980, *ApJ*, 238, 24
- Sanders D. B., Mirabel I. F., 1985, *ApJ*, 298, 31L
- Sansom A. E., Dotani T., Okada K., Yamashita A., Fabbiano G., 1996, *MNRAS*, 281, 48
- Schaaf R. et al., 1989, *ApJ*, 336, 722
- Schultz H., Komossa S., Berghöfer T., Boer B., 1998, *A&A*, 330, 823
- Serlemitsos P., Ptak A., Yaqoob T., 1996, in Eracleous M., Koratkar A., Leitherer C., Ho L., eds, *The physics of LINERS in view of recent observations*
- Smith et al., 1996, *ApJ*, 473, L21
- Soifer B. T. et al., 1987, *ApJ*, 320, 238
- Stark A. A. et al., 1992, *ApJS*, 79, 77
- Stewart G. C., Fabian A. C., Terlevich R. J., Hazard C., 1982, *MNRAS*, 200, 61
- Strickland D. K., Ponman T. J., Stevens I. R., 1997, *A&A*, 320, 378
- Tanaka Y., Inoue H., Holt S. S., 1994, *PASJ*, 46, 37L
- Telesco C. M., Gatley I., 1984, *ApJ*, 284, 557
- Trümper J., 1984, *Physica Scripta*, T7, 209
- Tsuru T. G., Awaki H., Koyama K., Ptak A., 1998, *PASJ*, 49, 619
- Vallée J. P., 1993, *MNRAS*, 264, 665
- Van der Kruit P. C., de Bruyn A.G., 1976, 48, 373
- Van Paradijs J., McClintock J.E., 1995, in Lewin W. H., van Paradijs J., van den Heuvel E. P. J., eds, *X-ray Binaries*. Cambridge Univ. Press, Cambridge
- Veilleux S., Osterbrock D. E., 1987, *ApJS*, 63, 295
- Voges W. et al., 1996, *IAU Circ.* 6420
- Watson M. G., Stanger V., Griffiths R. E., 1984, *ApJ*, 286, 144
- Wynn-Williams C. G., Hodapp K., Joseph R. D., Eales S. A., Becklin E. E., McLean I. S., Simons D. A., Wright G. S., 1991, *ApJ*, 377, 426
- Yaqoob T. et al., 1995, *ApJ*, 455, 508
- Yaqoob T. et al., 1997, *The ASCA ABC Guide*, v2.0, NASA/GSFC
- Zhao J. H., Anantharamaiah K. R., Goss W. M., Viallefond F., 1997, *ApJ*, 482, 186

This paper has been typeset from a $\text{T}_E\text{X}/\text{L}^{\text{A}}\text{T}_E\text{X}$ file prepared by the author.